Discontinuous Galerkin method for hyperbolic equations involving δ-singularities: negative-order norm error estimates and applications [1]

Yang Yang[2] and Chi-Wang Shu[3]

Abstract

In this paper, we develop and analyze discontinuous Galerkin (DG) methods to solve hyperbolic equations involving δ-singularities. Negative-order norm error estimates for the accuracy of DG approximations to δ-singularities are investigated. We first consider linear hyperbolic conservation laws in one space dimension with singular initial data. We prove that, by using piecewise k-th degree polynomials, at time t, the error in the $H^{-(k+2)}$ norm over the whole domain is $(k+1/2)$-th order, and the error in the $H^{-(k+1)}(\mathbb{R}\backslash\mathcal{R}_t)$ norm is $(2k+1)$-th order, where $\mathcal{R}_t$ is the pollution region due to the initial singularity with the width of order $\mathcal{O}(h^{1/2}\log(1/h))$ and h is the maximum cell length. As an application of the negative-order norm error estimates, we convolve the numerical solution with a suitable kernel which is a linear combination of B-splines, to obtain L^2 error estimate of $(2k+1)$-th order for the post-processed solution. Moreover, we also obtain high order superconvergence error estimates for linear hyperbolic conservation laws with singular source terms by applying Duhamel's principle. Numerical examples including an acoustic equation and the nonlinear rendez-vous algorithms are given to demonstrate the good performance of DG methods for solving hyperbolic equations involving δ-singularities.

Keywords: δ-singularities, discontinuous Galerkin method, negative-order norm error estimate, singular initial condition, singular source term, superconvergence, post-processing, rendez-vous algorithm.

[1]Research supported by DOE grant DE-FG02-08ER25863 and NSF grant DMS-1112700.

[2]Division of Applied Mathematics, Brown University, Providence, RI 02912. E-mail: yang_yang@brown.edu

[3]Division of Applied Mathematics, Brown University, Providence, RI 02912. E-mail: shu@dam.brown.edu

1 Introduction

In this paper, we develop and analyze discontinuous Galerkin (DG) methods for solving hyperbolic conservation laws

$$\begin{array}{ll} u_t + f(u)_x = g(x,t), & (x,t) \in R \times (0,T], \\ u(x,0) = u_0(x), & x \in R, \end{array} \tag{1.1}$$

where the initial condition u_0, or the source term $g(x,t)$, or the solution $u(x,t)$ contains δ-singularities. Such problems appear often in applications and are difficult to approximate numerically. Many numerical techniques rely on modifications with smooth kernels and hence may severely smear such singularities, leading to large errors in the approximation. On the other hand, the DG methods are based on weak formulations and can be designed directly to solve such problems without modifications, leading to very accurate results. We will provide numerical examples in this paper to demonstrate this advantage. More importantly, we will give rigorous error estimates for the DG methods on model problems involving δ-singularities.

The DG method, first introduced in 1973 by Reed and Hill [24], was generalized by Johnson and Pitkäranta to solve scalar linear hyperbolic equations with L^p-norm error estimates [18]. Subsequently, Cockburn et al. studied Runge-Kutta discontinuous Galerkin (RKDG) methods for hyperbolic conservation laws in a series of papers [10, 7, 8, 11]. In [9] Cockburn et al. proved high order superconvergence error estimates of DG methods including their divided differences for hyperbolic equations with smooth solutions in negative-order norms. They also demonstrated that the application of the post-processing techniques of Bramble and Schatz [1] can yield superconvergence in the strong L^2-norm. Other related works include [26, 29, 30, 25], where one-sided filter and local derivative post-processing were considered.

It is well known that generic solutions of hyperbolic equations are not smooth. Discontinuities or even δ-singularities may appear in the solutions. The DG methods have been shown to be L^2 stable for nonlinear hyperbolic equations with L^2 solutions which may contain discontinuities [15, 14]. A simple example of non-smooth solutions for hyperbolic equations

is the following problem

$$\begin{array}{ll} u_t + u_x = 0, & (x,t) \in R \times (0,T], \\ u(x,0) = u_0(x), & x \in R, \end{array} \tag{1.2}$$

where the initial solution $u_0(x)$ has compact support, has a discontinuity at $x = 0$, but is otherwise smooth. Clearly, the exact solution of (1.2) is discontinuous along the characteristic line $x = t$ and the numerical DG solution has spurious oscillations around this discontinuity line, which we refer to as the pollution region. There are not too many works in the literature studying error estimates of DG methods for problems with discontinuous solutions. The first work in this direction seems to be that of Johnson et al. [17, 18, 19] for DG methods in both space and time. They have shown that, with linear space-time elements, the width of the pollution region is of the size at most $\mathcal{O}(h^{1/2} \log 1/h)$. More recently, Cockburn and Guzmán [6] and Zhang and Shu [31] revisited this problem with the RKDG methods and obtained similar results. Especially, in [6], the left boundary of the pollution region is shown to be at most $\mathcal{O}(h^{2/3} \log(1/h))$ from the singularity for piecewise linear DG method with second order Runge-Kutta time discretization on uniform meshes. The first problem we consider in this paper is (1.2) with the initial condition $u_0(x)$ having a δ-singularity at $x = 0$. We consider semi-discrete DG method and use the result in [31] to prove the superconvergence results estimated in negative-order norms outside the pollution region. Further, by convolving the DG solution with a suitable kernel, the post-processed approximation is $(2k + 1)$-th order accurate in a region slightly smaller than the one we mentioned above. The rate of convergence agrees with that in [9], in which the initial datum $u_0(x)$ was assumed to be sufficiently smooth.

Hyperbolic conservation laws with source terms have been analyzed by several authors [3, 12, 20, 28, 21]. In particular, in [12], the authors studied the following problem

$$\begin{array}{ll} u_t + f(u)_x = g(x,t), & (x,t) \in R \times (0,T], \\ u(x,0) = u_0(x), & x \in R, \end{array} \tag{1.3}$$

where f is a smooth convex function ($f''(u) > 0$ for all u) and $g(x,t) = G_x(x,t)$ with G being a bounded, piecewise smooth function, and constructed L^∞ stable Godunov-type difference

schemes. In [27], Santos and de Oliveira studied hyperbolic conservation laws whose source terms contain δ-singularities, and investigated the convergence of numerical discretization by using a finite volume scheme. Later, they also considered a class of high resolution methods in [23]. In [22], Noussair studied the wave behavior of (1.3), where the source term also depends on u but not on the time variable t. We note that all these previous works did not provide any error estimates in the smooth region away from the singularities. In this paper, we investigate a simpler case by assuming $f(u) = u$ and $g(x,t) = G'(x)$ in the source term in (1.3), where $G(x)$ is a step function which does not depend on the time variable t. We show that by convolving the DG solution with a suitable kernel, the post-processed approximation turns out to be $(2k+1)$-th order superconvergent in the smooth region.

The organization of this paper is as follows. In section 2, we present preliminaries, including a brief introduction of the DG methods under consideration, some essential properties of finite element spaces as well as the post-processing technique. Sections 3 and 4 are the main body of this paper where we investigate the negative-order norm error estimates for hyperbolic conservation laws with singular initial condition and source term respectively. In section 5, we provide numerical evidences to validate our theoretical results. Moreover, additional numerical results for more general nonlinear equations will also be given to demonstrate the good performance of DG methods for problems containing δ-singularities. We will end in section 6 with some concluding remarks. A few technical details are contained in the appendix.

2 Preliminaries

In this section we consider the conservation law (1.1) on the interval $[0, 2\pi]$.

2.1 The DG scheme

First, we divide the computational domain $\Omega = [0, 2\pi]$ into N cells

$$0 = x_{\frac{1}{2}} < x_{\frac{3}{2}} < \cdots < x_{N+\frac{1}{2}} = 2\pi,$$

and denote

$$I_j = \left(x_{j-\frac{1}{2}}, x_{j+\frac{1}{2}}\right), \qquad x_j = \frac{1}{2}\left(x_{j-\frac{1}{2}} + x_{j+\frac{1}{2}}\right),$$

as the cells and cell centers respectively. $h_j = x_{j+\frac{1}{2}} - x_{j-\frac{1}{2}}$ denotes the length of each cell. We also denote $h = \max_j h_j$ as the length of the largest cell.

Next, we define

$$V_h = \{v : v|_{I_j} \in \mathcal{P}^k(I_j), j = 1, \cdots, N\}$$

as the finite element space, where $\mathcal{P}^k(I_j)$ denotes the space of polynomials in I_j of degree at most k. We also define

$$H_h^1 = \{\phi : \phi|_{I_j} \in H^1(I_j),\ \forall j\}.$$

The DG scheme we consider is the following: find $u_h \in V_h$, such that for any $v_h \in V_h$

$$((u_h)_t, v_h)_j = (f(u_h), (v_h)_x)_j - \hat{f}_{j+\frac{1}{2}} v_h^-|_{j+\frac{1}{2}} + \hat{f}_{j-\frac{1}{2}} v_h^+|_{j-\frac{1}{2}} + (g(x,t), v_h)_j, \tag{2.1}$$

where $(w, v)_j = \int_{I_j} wv dx$, and $v_h^-|_{j+\frac{1}{2}} = v_h(x^-_{j+\frac{1}{2}})$ denotes the left limit of the function v_h at $x_{j+\frac{1}{2}}$. Likewise for v_h^+. Moreover, the numerical flux $\hat{f}$ is a single valued function defined at the cell interfaces and in general depends on the values of the numerical solution u_h from both sides of the interfaces

$$\hat{f}_{i+\frac{1}{2}} = \hat{f}(u_h(x^-_{i+\frac{1}{2}}), u_h(x^+_{i+\frac{1}{2}})).$$

In general,we use monotone fluxes. For the linear case $f(u) = u$, we consider the upwind fluxes $\hat{f} = u_h^-$, then the numerical scheme (2.1) can be written as

$$((u_h)_t, v_h)_j = (u_h, (v_h)_x)_j - u_h^- v_h^-|_{j+\frac{1}{2}} + u_h^- v_h^+|_{j-\frac{1}{2}} + (g(x,t), v_h)_j \tag{2.2}$$

$$= -((u_h)_x, v_h)_j - [u_h] v_h^+|_{j-\frac{1}{2}} + (g(x,t), v_h)_j, \tag{2.3}$$

where $[u_h]_{j-\frac{1}{2}} = u_h(x^+_{j-\frac{1}{2}}) - u_h(x^-_{j-\frac{1}{2}})$ is the jump of u_h across $x_{j-\frac{1}{2}}$. We use the above two equations in sections 3 and 4 for the error estimates. We also define

$$\mathcal{H}_j(u_h, v_h) = (f(u_h), (v_h)_x)_j - \hat{f}_{j+\frac{1}{2}} v_h^-|_{j+\frac{1}{2}} + \hat{f}_{j-\frac{1}{2}} v_h^+|_{j-\frac{1}{2}}, \tag{2.4}$$

then the DG scheme can be written as $((u_h)_t, v_h)_j = \mathcal{H}_j(u_h, v_h) + (g(x,t), v_h)_j$. If we consider linear equations, (2.4) can be written as

$$\mathcal{H}_j(u_h, v_h) = (u_h, (v_h)_x)_j - u_h^- v_h^-|_{j+\frac{1}{2}} + u_h^- v_h^+|_{j-\frac{1}{2}}, \tag{2.5}$$

2.2 Norms

We now define some norms that we use throughout the paper.

Denote $\|u\|_{0,I_j}$ as the standard L^2-norm of u on cell I_j. For any natural number ℓ, we also define the norm and seminorm of the Sobolev space $H^\ell(I_j)$ as

$$\|u\|_{\ell,I_j} = \left\{ \sum_{0\le\alpha\le\ell} \|D^\alpha u\|_{0,I_j}^2 \right\}^{1/2}, \quad |u|_{\ell,I_j} = \|D^\ell u\|_{0,I_j}.$$

For convenience, if $\ell = 0$, the corresponding index will be omitted.

We also define the L^∞-norm and seminorm by

$$\|u\|_{\ell,\infty,I_j} = \max_{0\le\alpha\le\ell} \|D^k u\|_{\infty,I_j}, \quad |u|_{\ell,\infty,I_j} = \|D^\ell u\|_{\infty,I_j},$$

where $\|u\|_{\infty,I_j}$ is the standard L^∞-norm of u on cell I_j. Clearly, the L^∞-norm is stronger than the L^2-norm, and in one cell I_j, we have

$$\|u\|_{I_j} \le h_j^{1/2} \|u\|_{\infty,I_j}. \tag{2.6}$$

Moreover, we define the norms on $D = \cup_{j\in\Lambda} I_j$ for some index set Λ as follows:

$$\|u\|_{\ell,D} = \left(\sum_{j\in\Lambda} \|u\|_{\ell,I_j}^2 \right)^{1/2}, \quad \|u\|_{\ell,\infty,D} = \max_{j\in\Lambda} \|u\|_{\ell,\infty,I_j}.$$

For convenience, if $D = \Omega = [0, 2\pi]$, the corresponding index will be omitted.

Finally, the negative order Sobolev norm can be defined as

$$\|u\|_{-\ell,D} = \sup_{\phi\in C_0^\infty(D)} \frac{\int_D u(x)\phi(x)dx}{\|\phi\|_{\ell,D}}.$$

2.3 Properties of the finite element space

We use the classical inverse property.

Lemma 2.1 *Assume $v \in V_h$, then there exists a constant $C > 0$ independent of h and v such that*

$$\sum_{I_j \in D} \left(\left| v^-_{j+\frac{1}{2}} \right| + \left| v^+_{j-\frac{1}{2}} \right| \right) \leq C h^{-1/2} \|v\|_D, \tag{2.7}$$

where D can be either the single cell I_j or the whole computational domain Ω.

We define $\mathbb{P}_\ell(p)$ as the ℓ-th order L^2 projection of p into V_h, such that

$$(\mathbb{P}_\ell(p), v)_j = (p, v)_j \ , \quad \forall v \in \mathcal{P}^\ell(I_j). \tag{2.8}$$

In addition, if $\ell \geq 1$, we can also define two Gauss-Radau projections $\mathbb{P}_+$ and $\mathbb{P}_-$ as:

$$(\mathbb{P}_+(p), v)_j = (p, v)_j \ , \quad \forall v \in \mathcal{P}^{\ell-1}(I_j) \ , \quad \text{and} \quad \mathbb{P}_+(p)(x^+_{j-1/2}) = p(x^+_{j-1/2}), \tag{2.9}$$

$$(\mathbb{P}_-(p), v)_j = (p, v)_j \ , \quad \forall v \in \mathcal{P}^{\ell-1}(I_j) \ , \quad \text{and} \quad \mathbb{P}_-(p)(x^-_{j+1/2}) = p(x^-_{j+1/2}). \tag{2.10}$$

For the projection $\mathbb{P}_h$, which is either $\mathbb{P}_k$, $\mathbb{P}_+$ or $\mathbb{P}_-$, we denote the error operator by $\mathbb{P}_h^\perp = \mathbb{I} - \mathbb{P}_h$, where $\mathbb{I}$ is the identity operator. By the scaling argument, we obtain the following property [4].

Lemma 2.2 *Let $\mathbb{P}_h$ be a projection, either $\mathbb{P}_k$, $\mathbb{P}_-$ or $\mathbb{P}_+$. For any sufficiently smooth function $p(x)$, there exists a positive constant C independent of h and p, such that*

$$\|\mathbb{P}_h^\perp p\|_D + h\|\partial_x(\mathbb{P}_h^\perp p)\|_D + h^{1/2}\|\mathbb{P}_h^\perp p\|_{\infty,D} \leq C h^{k+1} |p|_{k+1,D}, \tag{2.11}$$

where D can be either the single cell I_j or the whole computational domain Ω.

Now, we consider the projection of functions depending not only on the spatial variable x but also on the time variable t. Suppose $u(x,t)$ is a function differentiable and integrable with respect to t, also assume t_1 and t_2 are two real values such that $t_1 < t_2$, then we have

$$\mathbb{P}_h \left(u_t(x,t) \right) = \left(\mathbb{P}_h u(x,t) \right)_t , \qquad \text{and} \qquad \mathbb{P}_h \left(\int_{t_1}^{t_2} u(x,t) dt \right) = \int_{t_1}^{t_2} (\mathbb{P}_h u(x,t)) dt. \tag{2.12}$$

Because of this, we do not need to distinguish $\mathbb{P}_h(u_t(x,t))$ and $(\mathbb{P}_h u(x,t))_t$, and can simply denote them as $\mathbb{P}_h u_t$.

2.4 Properties of the DG spatial discretization

In this subsection, we present some basic properties about the bilinear form $\mathcal{H}_j$ and the L^2 stability condition [5]. We consider the linear case, namely (1.1) with $f(u) = u$.

Lemma 2.3 *Suppose u_h is the DG numerical solution which satisfies* (2.2) *in each cell with $g = 0$. By using the upwind flux, we have*

$$\|u_h(T)\|^2 + \int_0^T \sum_{1\le j\le N} [u_h(t)]^2_{j+1/2}\, dt \le \|u_h(0)\|^2. \tag{2.13}$$

Lemma 2.4 *Suppose $v_h \in V_h$ and $q(x) \in H_h^1$, the two Gauss-Radau projections satisfy the following properties*

$$\mathcal{H}_j(\mathbb{P}_-^\perp q(x), v_h) = 0, \quad \textit{and} \quad \mathcal{H}_j(v_h, \mathbb{P}_+^\perp q(x)) = 0. \tag{2.14}$$

If we define $(u_h, v_h) = \sum_j (u_h, v_h)_j$ and $\mathcal{H}(p, q) = \sum_j \mathcal{H}_j(p, q)$, then

Lemma 2.5 *Suppose $p(x) \in H_h^1$ and $v_h \in V_h$, there holds*

$$\mathcal{H}(\mathbb{P}_-^\perp p(x), v_h) = 0, \quad \textit{and} \quad \mathcal{H}(v_h, \mathbb{P}_+^\perp p(x)) = 0. \tag{2.15}$$

2.5 Post-processing

Now, we proceed to describe the type of post-processing to be considered, following Bramble and Schatz [1]. Let χ be the indicator function of the interval $(-\frac{1}{2}, \frac{1}{2})$, We define recursively the functions $\psi^{(l)}$ as

$$\psi^{(1)} = \chi, \qquad \psi^{(n+1)} = \psi^{(n)} * \psi^{(1)}, \text{ for } n \ge 1.$$

We post-process the numerical solution by convolving it with a kernel $K^{(\nu,l)}(x)$ which satisfies the following properties:

(1) It has a compact support.

(2) It reproduces polynomials p of degree $\nu - 1$ by convolution: $K^{(\nu,l)} * p = p$.

(3) It is a linear combination of B-splines and is of the form

$$K^{(\nu,l)}(x) = \sum_{\gamma\in\mathbb{Z}} k_\gamma^{\nu,l} \psi^{(l)}(x - \gamma).$$

The weights $k_\gamma^{\nu,l} \in \mathbb{R}$ are chosen so that (2) is satisfied. See [1, 9] for more details. We also define $K_H^{(\nu,l)}(x) = K^{(\nu,l)}(x/H)/H$ and $\psi_H^{(l)}(x) = \psi^{(l)}(x/H)/H$ and it is not difficult to verify that

$$D^\alpha(\psi^{(\beta)}) * v = \psi_H^{(\beta-\alpha)} * \partial_H^\alpha v,$$

where $\partial_H v(x) = \frac{1}{H}(v(x+\frac{1}{2}H) - v(x-\frac{1}{2}H))$. In general, we take $H = nh,\ n = 1, 2, \cdots$. This property is really important because it allows us to express derivatives of the convolution with the kernel in terms of simple difference quotients.

2.6 An approximation result

In this subsection, we investigate the relationship between $u - K_h^{2k+2,k+1} * u_h$ and the negative-order norm estimates of divided differences of the error $u - u_h$.

Theorem 2.1 (Bramble and Schatz [1]) *Suppose the kernel $K_h^{\nu,l}$ satisfies the properties listed in section 2.5. Let v be a function in $L^2(\Omega_1)$, where Ω_1 is an open set in Ω, and u be a function in $H^\nu(\Omega_1)$. Further assume Ω_0 to be an open set in Ω_1 such that $\Omega_0 + 2supp(K_h^{\nu,l}) \subset\subset \Omega_1$. Then we have*

$$\|u - K_h^{\nu,l} * v\|_{\Omega_0} \le \frac{h^\nu}{\nu!} C_1 |u|_{\nu,\Omega_1} + C_1 C_2 \sum_{\alpha \le l} \|\partial_h^\alpha (u - v)\|_{-l,\Omega_1},$$

where $C_1 = \sum_{\gamma \in \mathbb{Z}} |k_\gamma^{\nu,l}|$ and C_2 only depends on Ω_0, Ω_1, ν, and l.

There is a straightforward corollary.

Corollary 2.1 *Suppose the conditions in theorem 2.1 are satisfied. Further assume that $\|\partial_h^\alpha (u - v)\|_{-l,\Omega_1} \le Ch^\mu$ is valid for all $\alpha \le l$ and $\nu \ge \mu$. Then we have*

$$\|u - K_h^{\nu,l} * v\|_{\Omega_0} \le Ch^\mu,$$

where C only depends on Ω_0, Ω_1, ν, and l.

3 Singular initial condition

In this section we consider problem (1.2) and use upwind fluxes. We first state the main results in theorem 3.1 and then give the proofs. We provide the negative-order norm error estimates in the whole space as well as in the region away from the singularities.

3.1 Main results

The following lemma is the semi-discrete version of the result in Zhang and Shu [31]. For completeness we will give its proof in the appendix.

Lemma 3.1 *Let u be the exact solution of the initial value problem (1.2), where the initial condition $u_0(x) \in C^{k+2}$ except for one singularity at $x = 0$. Let u_h be the solution of the DG method (2.2) at time T, where the finite element space V_h is made up of the piecewise polynomials of degree $k \geq 1$. Suppose h is the maximum cell length. Then there holds the following error estimate*

$$\|u(T) - u_h(T)\|_{\Omega \backslash \mathcal{R}_T} \leq Ch^{k+1}, \tag{3.1}$$

where $\mathcal{R}_T = (T - Ch^{1/2}\log(1/h), T + Ch^{1/2}\log(1/h))$, and the bounding constant $C > 0$ does not depend on h.

We will use lemma 3.1 to prove the following theorem.

Theorem 3.1 *Suppose $u \in C^{2k+2}$ and the conditions of Lemma 3.1 are satisfied. Then by taking $\Omega_0 + 2supp(K_h^{2k+2,k+1}) \subset\subset \Omega_1 \subset\subset \Omega \backslash \mathcal{R}_T$, we have*

$$\|u(T) - u_h(T)\|_{-(k+1)} \leq Ch^k, \tag{3.2}$$

$$\|u(T) - u_h(T)\|_{-(k+2)} \leq Ch^{k+1/2}, \tag{3.3}$$

$$\|u(T) - u_h(T)\|_{-(k+1),\Omega_1} \leq Ch^{2k+1}, \tag{3.4}$$

$$\|u(T) - K_h^{2k+2,k+1} * u_h(T)\|_{\Omega_0} \leq Ch^{2k+1}, \tag{3.5}$$

where the positive constant C does not depend on h. Here the mesh is assumed to be uniform for (3.5) but can be regular and non-uniform for the other three inequalities.

Remark 3.1 *To obtain equation* (3.5)*, we have to assume the mesh is uniformly distributed, that is* $h_j = h$, $\forall\ j$. *This is because of the negative-order norm estimates of the divided differences. Actually, we denote* $w = \partial_h u$ *and* $w_h = \partial_h u_h$. *Clearly,* w *satisfies equation* (1.2) *with initial condition* $w(x,0) = \partial_h u(x,0)$. *If we shift the mesh by* $\frac{h}{2}$*, then* w_h *satisfies numerical scheme (2.2). By the same analysis for the proof of equation* (3.4)*, we obtain*

$$\|\partial_h(u-u_h)\|_{-(k+1),\Omega_1} = \|w-w_h\|_{-(k+1),\Omega_1} \le Ch^{2k+1}.$$

The estimates for higher order divided differences can be obtained by exactly the same line in this remark. Therefore, equation (3.5) *follows directly from Corollary 2.1.*

Remark 3.2 *The error estimates in* $-(k+1)$*-th order norm are used for problems with singular initial conditions while the estimates in* $-(k+2)$*-th order norm are used for problems with singular source terms.*

3.2 A proof of Theorem 3.1

In this subsection, we give the initial discretization and prove the first three estimates in Theorem 3.1.

3.2.1 Initial discretization

From now on, we assume the δ-singularity of the initial datum is contained in cell I_i. For simplicity, we also assume the singularity is concentrated at 0, denoted as $\delta(x)$. We apply the L^2 projection $\mathbb{P}_k$ to discretize the initial condition to obtain $\|u_h(0)\| \le Ch^{-1/2}$. At $t = 0$, for any function $\phi \in C_0^\infty(\Omega)$, we have, for the cell I_i which contains the δ-singularity,

$$\begin{aligned}(u-u_h,\phi)_i &= (u-u_h,\phi-\mathbb{P}_k\phi)_i\\ &= (u,\phi-\mathbb{P}_k\phi)_i\\ &\le \|\phi-\mathbb{P}_k\phi\|_{\infty,I_i}\\ &\le Ch^{k+\frac{1}{2}}|\phi|_{k+1,I_i}.\end{aligned}$$

In other cells, following the same analysis above, we have

$$(u-u_h,\phi)_j=(u-\mathbb{P}_k u,\phi-\mathbb{P}_k\phi)_j\le Ch^{2k+2}|u_0|_{k+1,I_j}|\phi|_{k+1,I_j}. \tag{3.6}$$

3.2.2 The $-(k+1)$-th order error estimate on Ω

In this subsection, we proceed to prove equation (3.2). The proof mostly follows [9]. We begin by considering the solution to the dual problem: Find a function ϕ such that $\phi(\cdot,t)$ satisfies

$$\begin{aligned}&\phi_t+\phi_x=0, && (x,t)\in\Omega\times(0,T),\\ &\phi(x,T)=\Phi(x), && x\in\Omega.\end{aligned} \tag{3.7}$$

Assuming Φ is an arbitrary function in $C_0^\infty(\Omega)$, we have, following [9],

$$\begin{aligned}(u(T)-u_h(T),\Phi)&=(u-\mathbb{P}_k u,\phi)(0)-\int_0^T[((u_h)_t,\phi)+(u_h,\phi_t)]dt &(3.8)\\ &=(u-\mathbb{P}_k u,\phi)(0)-\int_0^T\sum_{j=1}^N[u_h](\phi-\mathbb{P}_k\phi)^+|_{j-\frac12} &(3.9)\\ &\le Ch^{k+1/2}|\Phi|_{k+1}+Ch^{k+1/2}|\Phi|_{k+1}\int_0^T\left(\sum_{j=1}^N[u_h]^2_{j-\frac12}\right)^{1/2}dt.\end{aligned}$$

Using Cauchy-Schwarz inequality and lemma 2.3, we have

$$\begin{aligned}\int_0^T\left(\sum_{j=1}^N[u_h]^2_{j-\frac12}\right)^{1/2}dt&\le T^{1/2}\left(\int_0^T\sum_{j=1}^N[u_h]^2_{j-\frac12}dt\right)^{1/2}\\ &\le T^{1/2}\|u_h(0)\|\\ &\le CT^{1/2}h^{-1/2}.\end{aligned}$$

Combining the above, we can see

$$\begin{aligned}\|u(T)-u_h(T)\|_{-(k+1)}&=\sup_{\Phi\in C_0^\infty(\Omega)}\frac{(u(T)-u_h(T),\Phi)}{\|\Phi\|_{k+1}}\\ &\le\sup_{\Phi\in C_0^\infty(\Omega)}\frac{Ch^{k+1/2}|\Phi|_{k+1}+CT^{1/2}h^k|\Phi|_{k+1}}{\|\Phi\|_{k+1}}\\ &\le CT^{1/2}h^k+Ch^{k+1/2}.\end{aligned}$$

Now, we consider the extension to higher dimensions. The proof of the following corollary is straightforward and is similar to the one-dimensional case, and is thus omitted.

Corollary 3.1 *Let Ω be an open set in $\mathbb{R}^d$, and u be the exact solution of the following initial value problem*

$$\begin{aligned} &u_t + \textstyle\sum_{j=1}^{d} u_{x_j} = 0, && (x,t) \in \Omega \times (0,T], \\ &u(x,0) = \delta(f(x)), && x \in \Omega, \end{aligned}$$

where $f(x) : \mathbb{R}^d \to \mathbb{R}$ is a smooth function. Denote $\Gamma_h = \{K\}$ as a regular triangulation of $\mathbb{R}^d$, whose elements K are open and have diameter h_K less than or equal to h. In each K, denote ∂K_- and ∂K_+ as the inflow and outflow edges respectively. Let u_h be the DG approximation which satisfies

$$(u_{ht}, v_h)_K = \sum_{i=1}^{d} (u_h, (v_h)_{x_i})_K + \sum_{i=1}^{d} (u_h^-, v_h^+)_{\partial K_-} - \sum_{i=1}^{d} (u_h^-, v_h^-)_{\partial K_+}, \quad v_h \in V_h,$$

where the finite element space V_h is made up of the piecewise polynomials of degree $k \geq 1$. Suppose the total measure of the cells which contain δ-singularities initially is mh, then there holds the following estimate

$$\|u(T) - u_h(T)\|_{-k-1} \leq C\sqrt{m} T^{1/2} h^k + C h^{k+d/2}, \tag{3.10}$$

where the bounded constant $C > 0$ does not depend on h or T.

3.2.3 The $-(k+2)$-th order error estimate on Ω

In this subsection, we prove equation (3.3). To do so, we apply $\mathbb{P}_+$ to estimate the term $(u_{ht}, \phi) + (u_h, \phi_t)$. By using equation (2.4) and lemma 2.5, we obtain

$$\begin{aligned} (u_{ht}, \phi) + (u_h, \phi_t) &= (u_{ht}, \mathbb{P}_+^{\perp}\phi) + (u_{ht}, \mathbb{P}_+\phi) - (u_h, \phi_x) \\ &= (u_{ht}, \mathbb{P}_+^{\perp}\phi) + \mathcal{H}(u_h, \mathbb{P}_+\phi) - \mathcal{H}(u_h, \phi) \\ &= (u_{ht}, \mathbb{P}_+^{\perp}\phi). \end{aligned} \tag{3.11}$$

Integrating in t, we obtain

$$\int_0^T (u_{ht}, \phi) + (u_h, \phi_t) dt = (u_h, \mathbb{P}_+^{\perp}\phi)(T) - (u_h, \mathbb{P}_+^{\perp}\phi)(0) - \int_0^T (u_h, \mathbb{P}_+^{\perp}\phi_t) dt. \tag{3.12}$$

Applying lemma 2.3, we have

$$\int_0^T (u_{ht}, \phi) + (u_h, \phi_t) dt \leq \|u_h(0)\| \ \left(\|(\mathbb{P}_+^{\perp}\phi)(0)\| + \|(\mathbb{P}_+^{\perp}\phi)(T)\| \right) + \int_0^T \|u_h(0)\| \ \|\mathbb{P}_+^{\perp}\phi_t(t)\| dt$$

$$\leq C\|u_h(0)\| \left(h^{k+1}|\Phi|_{k+1} + \int_0^T h^{k+1}|\Phi|_{k+2} dt \right)$$
$$\leq C(1+T)h^{k+1}\|u_h(0)\|\|\Phi\|_{k+2}.$$

From the above we can see

$$\begin{aligned}
\|u(T) - u_h(T)\|_{-(k+2)} &= \sup_{\Phi \in C_0^\infty(\Omega)} \frac{(u(T) - u_h(T), \Phi)}{\|\Phi\|_{k+2}} \\
&\leq \sup_{\Phi \in C_0^\infty(\Omega)} \frac{Ch^{k+\frac{1}{2}}|\Phi|_{k+1} + C(1+T)h^{k+\frac{1}{2}}\|\Phi\|_{k+2}}{\|\Phi\|_{k+2}} \\
&\leq C(1+T)h^{k+\frac{1}{2}}.
\end{aligned}$$

3.3 The negative-order error estimate on $\Omega_1 \subset\subset \Omega \backslash \mathcal{R}_T$

In this subsection we proceed to prove equation (3.4). To estimate the negative-order norm of $u - u_h$ at time T on Ω_1, we need to assume $\Phi \in C_0^\infty(\Omega_1)$ instead of $C_0^\infty(\Omega)$. Moreover, we also assume the exact solution $u \in C(\Omega)$, this is because we are allowed to modify the exact solution in the cell which contains the δ-singularity, keeping the numerical solution u_h untouched. More details of this assumption can be found in [31, 6] or Appendix A.2. Therefore, in equation (3.9), we have

$$\begin{aligned}
\sum_{j=1}^{N} [u_h](\phi - \mathbb{P}_k\phi)^+|_{j-\frac{1}{2}} &= \sum_{j=1}^{N} [u_h - \mathbb{P}_k u + \mathbb{P}_k u - u](\phi - \mathbb{P}_k\phi)^+|_{j-\frac{1}{2}} \\
&\leq Ch^k \left(\|u - \mathbb{P}_k u\|_{\Omega_1} + \|\mathbb{P}_k u - u_h\|_{\Omega_1} \right) |\phi|_{k+1} \\
&\leq Ch^k \left(\|u - \mathbb{P}_k u\|_{\Omega_1} + \|u - u_h\|_{\Omega_1} \right) |\phi|_{k+1} \\
&\leq Ch^{2k+1}|\phi|_{k+1},
\end{aligned}$$

where, we use lemmas 2.1 and 2.2 in the second inequality and lemma 3.1 in the last one. Plugging the above estimate into (3.9), we have

$$(u(T) - u_h(T), \Phi) \leq (u - \mathbb{P}_k u, \phi)(0) + Ch^{2k+1}|\phi|_{k+1}. \tag{3.13}$$

By using equation (3.6), we obtain the estimate we want

$$\begin{aligned}\|u(T)-u_h(T)\|_{-(k+1),\Omega_1} &= \sup_{\Phi\in C_0^\infty(\Omega_1)} \frac{(u(T)-u_h(T),\Phi)}{\|\Phi\|_{k+1}} \\ &\le \sup_{\Phi\in C_0^\infty(\Omega_1)} \frac{Ch^{2k+1}\|\Phi\|_{k+1}+Ch^{2k+2}\|\Phi\|_{k+1}}{\|\Phi\|_{k+1}} \\ &\le Ch^{2k+1},\end{aligned}$$

where the constant $C>0$ is independent of h.

4 Singular source term

In this section, we briefly discuss a linear inhomogeneous evolution equation of a function

$$u(x,t):\Omega\times(0,\infty)\to\mathbb{R}$$

of the form

$$\begin{cases} u_t(x,t)+Lu(x,t)=f(x,t), & (x,t)\in\Omega\times(0,\infty), \\ u(x,0)=0, & x\in\Omega, \end{cases} \tag{4.1}$$

with L being a linear differential operator that does not involve time derivatives. If we multiply the above equation by a smooth function $\phi(x,t)$, then integrate over space and time, we obtain

$$\int_0^\infty\int_\Omega [\phi u_t+\phi Lu]\,dxdt=\int_0^\infty\int_\Omega f(x,t)\phi(x,t)dxdt.$$

Integrating by parts and assuming zero boundary condition, we have

$$\int_0^\infty\int_\Omega [u\phi_t+uL^*\phi]\,dxdt+\int_0^\infty\int_\Omega f(x,t)\phi(x,t)dxdt=0, \tag{4.2}$$

where L^* is the dual operator of L.

Definition 4.1 *The function $u(x,t)$ is called a weak solution of the equation* (4.1)*, if* (4.2) *holds for all functions $\phi\in C_0^1(\Omega\times\mathbb{R}^+)$.*

4.1 Duhamel's principle

Now, we consider linear hyperbolic conservation laws with source terms. To deal with such problems we apply Duhamel's principle, which is applicable to linear parabolic and hyperbolic partial differential equations (PDE) and yields an integral representation in terms of the solutions of more tractable PDEs.

Lemma 4.1 (Duhamel's principle) *The solution to equation* (4.1) *is*

$$u(x,t) = \int_0^t (P^s f)(x,t)ds,$$

where $P^s f$ *is the solution of the problem*

$$\begin{cases} P_t(x,t) + LP(x,t) = 0, & (x,t) \in \Omega \times (s,\infty), \\ P(x,s) = f(x,s), & x \in \Omega. \end{cases} \tag{4.3}$$

Notice that $P^s f$ is the solution to the homogeneous PDE with the source term f serving as the initial condition at time $t = s$. To prove the lemma, we can simply check that the expression of u in the lemma satisfies equation (4.1). More details and a proof can be found in [16], in which the PDE is a second order wave equation. The above lemma requires suitable regularity of u, however, the Duhamel's principle is also valid in the following weak sense.

Lemma 4.2 *Suppose* $u(x,t)$ *is the weak solution of equation* (4.1)*, then*

$$u(x,t) = \int_0^t (P^s f)(x,t)ds$$

in the sense of distribution, where $P^s f$ *is the weak solution of equation* (4.3)*.*

The proof directly follows from the definition of the weak solution and the proof of the Duhamel's principle, so we omit it here.

Finally, we extend the Duhamel's principle to the DG schemes. For simplicity, we only consider the following equation

$$\begin{cases} u_t(x,t) + u_x(x,t) = \delta(x), & (x,t) \in \Omega \times (0,T), \\ u(x,0) = u_0(x), & x \in \Omega, \end{cases} \tag{4.4}$$

with $u_0 = 0$. For general smooth $u_0(x)$, the same result can be obtained by superposition. We define the finite element approximation $u_h : [0, T] \to V_h$ as the solution to

$$\begin{aligned} &(u_{ht}, \chi)_j = \mathcal{H}_j(u_h, \chi) + (\delta(x), \chi)_j, \quad \forall \chi \in V_h, \\ &u_h(0) = 0, \end{aligned} \tag{4.5}$$

where $\mathcal{H}_j(\cdot, \cdot)$ is the same DG bilinear form as we defined in (2.5). Then the semi-discrete version of Duhamel's principle is given in Lemma 4.3.

Lemma 4.3 *The solution of equation* (4.5) *can be written in the form* $u_h = \int_0^t p^s(x,t)ds$ *where* $p^s(x,t)$ *is the solution of the following scheme: find* $p \in V_h$ *such that*

$$\begin{aligned} &(p_t, \chi)_j = \mathcal{H}_j(p, \chi), \quad \forall \chi \in V_h, \\ &p(s) = \mathbb{P}_k \delta(x). \end{aligned} \tag{4.6}$$

The proof is straightforward, since u_h in (4.5) and $\int_0^t p^s(x,t)ds$ share the same initial condition and the same system of ODEs, noticing the fact that $(\mathbb{P}_k\delta, \chi) = (\delta, \chi)$.

In what follows, we would like to rewrite the inhomogeneous equations (4.4) and (4.5) into homogeneous ones (4.11) and (4.6) by using lemma 4.2 and lemma 4.3 respectively. Then we apply the estimates of $P^s f - p^s$, which have been given in theorem 3.1, to prove the main result in this section, theorem 4.1.

4.2 Error estimates

In this subsection, we first state the main result theorem 4.1 and then give the proof.

Theorem 4.1 *Suppose* u *is the exact solution of equation* (4.4)*, and* u_h *is the numerical solution which satisfies* (4.5)*. Denote* $\mathcal{R}_T = I_i \cup (T - C\log(1/h)h^{1/2}, T + C\log(1/h)h^{1/2})$*, where* I_i *is the cell which contains the concentration of the* δ*-singularity on the source term. Then we have the following estimates*

$$\|u(T) - u_h(T)\|_{-(k+1)} \leq Ch^k, \tag{4.7}$$

$$\|u(T) - u_h(T)\|_{-(k+2)} \leq Ch^{k+1/2}, \tag{4.8}$$

$$\|u - u_h\|_{-(k+1),\Omega_1} \leq Ch^{2k+1}, \tag{4.9}$$

$$\|u(T) - K_h^{2k+2,k+1} * u_h(T)\|_{\Omega_0} \leq Ch^{2k+1}, \tag{4.10}$$

where $\Omega_0 + 2supp(K_h^{2k+2,k+1}) \subset\subset \Omega_1 \subset\subset \mathbb{R}\backslash\mathcal{R}_T$. *Here the mesh is assumed to be uniform for (4.10) but can be regular and non-uniform for the other three inequalities.*

Remark 4.1 *As mentioned in remark 3.1, equation* (4.10)*, which requires uniform meshes, follows from equation* (4.9)*. Moreover, we also skip the proofs of equations* (4.7) *and* (4.8)*, since they follow easily from equations* (3.2) *and* (3.3) *in theorem 3.1.*

Now we proceed to prove equation (4.9). Denote v^s as the exact solution of the following equation

$$\begin{array}{ll} u_t + u_x = 0, & (x,t) \in \Omega \times (s,T], \\ u(x,s) = \delta(x), & x \in \Omega, \end{array} \tag{4.11}$$

and v_h^s as the solution of the numerical scheme (4.6). For convenience, if $s = 0$, the superscript will be omitted. We consider the dual problem defined the same as equation (3.7). By lemma 4.3 and lemma 4.2, we have

$$(u - u_h, \Phi)(T) = \int_0^T (v^s - v_h^s, \Phi)(T) ds. \tag{4.12}$$

By using equation (3.8) and equation (3.11), and noticing the fact that v_h is the L^2 projection of v at $t = 0$, we obtain

$$(v^s - v_h^s, \Phi)(T) = ((v - v_h)(0), \mathbb{P}_+^\perp \phi(s)) - \int_s^T (v_{ht}(t-s), \mathbb{P}_+^\perp \phi(t)) dt,$$

which further yields

$$(u - u_h, \Phi)(T) = \Pi_1 - \Pi_2,$$

where $\Pi_1 = \int_0^T ((v - v_h)(0), \mathbb{P}_+^\perp \phi(s)) ds$, and $\Pi_2 = \int_0^T \int_s^T (v_{ht}(t-s), \mathbb{P}_+^\perp \phi(t)) dt ds$. We first consider the second term,

$$\begin{aligned} \Pi_2 &= -\int_0^T \int_0^t ((v_h)_s(t-s), \mathbb{P}_+^\perp \phi(t)) ds dt \\ &= \int_0^T (v_h(t) - v_h(0), \mathbb{P}_+^\perp \phi(t)) dt. \end{aligned}$$

Therefore,

$$\begin{aligned}(u-u_h,\Phi)(T) &= \int_0^T (v(0),\mathbb{P}_+^{\perp}\phi(s))ds - \int_0^T (v_h(t),\mathbb{P}_+^{\perp}\phi(t))dt \\ &= G_1 - G_2.\end{aligned}$$

We claim $G_1 = 0$. Actually, for any $\tau \in I_i$, $\int_\tau^{T+\tau} \Phi(x)dx$ does not depend on τ, since $\Phi(x)$ vanishes in the neighborhood of $x = 0$ and $x = T$. Therefore,

$$G_1 = \left(\delta(x),\mathbb{P}_+^{\perp}\int_0^T \phi(x,s)ds\right) = \left(\delta(x),\mathbb{P}_+^{\perp}\int_x^{x+T} \Phi(y)dy\right)_i = 0.$$

Now, we only need to estimate G_2. Since

$$(v_h(t),\mathbb{P}_+^{\perp}\phi(t)) = (v_h(t) - v(t) + v(t) - \mathbb{P}_{k-1}v,\mathbb{P}_+^{\perp}\phi(t)),$$

by lemma 3.1 and lemma 2.2, we have $G_2 \le Ch^{2k+1}|\phi|_{k+1}$. Finally, we obtain

$$\|u-u_h\|_{-(k+1),\Omega_1} \le Ch^{2k+1}$$

and complete the proof of theorem 4.1.

5 Numerical examples

In this section, we provide numerical experiments to demonstrate our theoretical results for the post-processor in the first two subsections and to illustrate the good performance of the DG schemes for nonlinear rendez-vous algorithms which involve δ-singularities in the last one. We denote by d the distance between the singularities and the region under consideration. In all the figures, if not otherwise stated, the numerical solutions are plotted using six Gaussian points in each cell.

5.1 Singular initial condition

Example 1. We solve the following problem

$$\begin{array}{ll} u_t + u_x = 0, & (x,t) \in [0,\pi]\times(0,1], \\ u(x,0) = \sin(2x) + \delta(x-0.5), & x \in [0,\pi], \end{array} \tag{5.1}$$

with periodic boundary condition $u(0,t) = u(\pi,t)$. Clearly, the exact solution is

$$u(x,t) = \sin(2x - 2t) + \delta(x - t - 0.5).$$

We use ninth order SSP Runge-Kutta discretization in time [13] and take the time step $\Delta t = 0.1h$. We test the example by using $\mathcal{P}^k$ polynomials with $k = 1, 2, 3$ on uniform meshes, and compute the L^2-norm of the error after post-precessing in the region away from the singularity at $t = 0.5$. By taking $d = 0.2$, the region under consideration is $[0, 0.8] \cup [1.2, \pi]$. In table 5.1, we can observe at least $(2k+1)$-th order convergence. Moreover, we observe that the rate of convergence settles to the asymptotic value when the total number of cells is around $\frac{dN}{\pi} = \frac{0.2\times 500}{\pi} \approx 30$, no matter which degree of polynomials we use. The initial discretization is obtained by taking the L^2 projection.

Table 5.1: L^2-norm of the error between the numerical solution and the exact solution for equation (5.1) after post-processing in the region away from the singularity.

		$\mathcal{P}^1$ polynomial		$\mathcal{P}^2$ polynomial		$\mathcal{P}^3$ polynomial	
N	d	error	order	error	order	error	order
200	0.2	6.88E-05	-	8.40e-07	-	1.48E-09	-
300	0.2	1.41E-05	3.92	3.56e-10	19.2	3.98E-13	20.3
400	0.2	5.89E-06	3.02	1.98e-11	10.1	4.42E-16	23.7
500	0.2	3.01E-06	3.01	6.13e-12	5.25	7.49E-17	7.95
600	0.2	1.74E-06	3.00	2.37e-12	5.21	1.76E-17	7.94

Figure 5.1 shows the numerical solution with and without post-processing. We use $\mathcal{P}^2$ polynomials and take $h = 0.01$. From the figure we can observe some localized oscillations near the discontinuity and the post-processor does not smear the singularity too much.

Example 2. We consider the following two dimensional problem

$$\begin{aligned} &u_t + u_x + u_y = 0, && (x,y,t) \in [0,2\pi] \times [0,2\pi] \times (0,1], \\ &u(x,0) = \sin(x+y) + \delta(x+y-2\pi), && (x,y) \in [0,2\pi] \times [0,2\pi], \end{aligned} \tag{5.2}$$

with periodic boundary condition. Clearly, the exact solution is

$$u(x,t) = \sin(x + y - 2t) + \delta(x + y - 2t) + \delta(x + y - 2t - 2\pi).$$

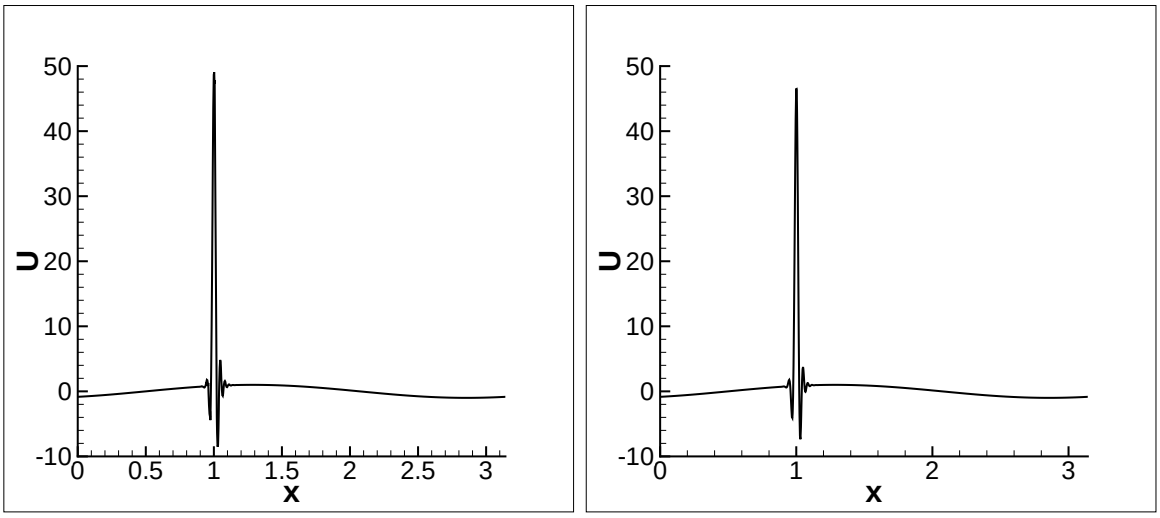

Figure 5.1: Numerical solution for (5.1) at $t = 0.5$ with (right) and without (left) post-processing.

We use $\mathcal{Q}^k$ polynomial approximation spaces with $k = 1$ and 2, where $\mathcal{Q}^k$ is the space of tensor product polynomials of degree at most $k \geq 0$. We also apply the same time discretization as in example 1 and compute the L^2-norm of the error after post-precessing in the region away from the singularity at $t = 0.5$. Moreover, we take $d = 0.4$. In table 5.2, we can observe $(2k + 1)$-th order convergence.

Table 5.2: L^2-norm of the error between the numerical solution and the exact solution for equation (5.2) after post-processing in the region away from the singularity.

		$\mathcal{Q}^1$ polynomial		$\mathcal{Q}^2$ polynomial	
N	d	error	order	error	order
400	0.4	2.60E-05	-	3.23e-08	-
500	0.4	1.24E-05	3.32	2.47e-10	20.0
600	0.4	7.16E-06	3.01	1.19e-11	16.6
700	0.4	4.50E-06	3.01	5.11e-12	5.47
800	0.4	3.01E-06	3.02	2.53e-12	5.29

It appears that similar results are valid in two dimensions. However, the technique of proof in this paper, in particular the part related to the special projections in (2.9) and (2.10), does not seem to be easily extendable to two dimensions.

Moreover, figure 5.2 shows the numerical solution by plotting the numerical cell averages. We use $\mathcal{Q}^2$ polynomials and take $N = 100$. From the figure we can observe two lines of δ-singularities.

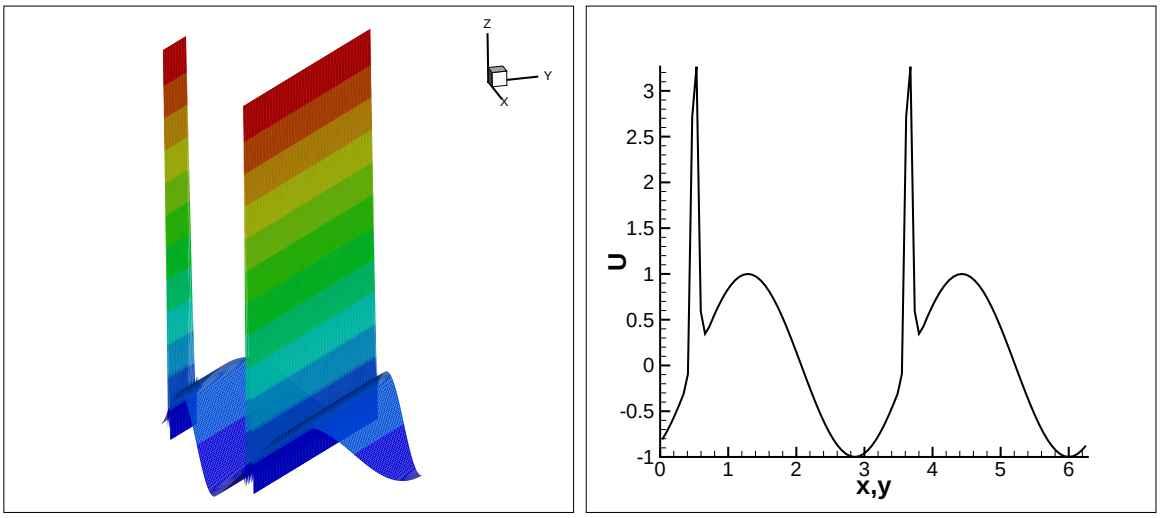

Figure 5.2: Numerical solution (left) and the cut plot along $x = y$ (right) for (5.2) at $t = 0.5$.

Example 3. Even though the theory in this paper is given only for scalar linear equations for simplicity, it generalizes to linear systems in a straightforward way. We solve the following linear system

$$\begin{array}{ll} u_t - v_x = 0, & (x,t) \in [0,2] \times (0,0.4], \\ v_t - u_x = 0, & (x,t) \in [0,2] \times (0,0.4], \\ u(x,0) = \delta(x-1), v(x,0) = 0, & x \in [0,2]. \end{array} \tag{5.3}$$

Clearly, the exact solution (the Green's function) is

$$u(x,t) = \frac{1}{2}\delta(x-1-t) + \frac{1}{2}\delta(x-1+t), \quad v(x,t) = \frac{1}{2}\delta(x-1+t) - \frac{1}{2}\delta(x-1-t).$$

We use third order SSP Runge-Kutta discretization in time [13] and take the time step $\Delta t = 0.1h$. Figure 5.3 shows the numerical solutions at $t = 0.4$ with $\mathcal{P}^3$ polynomials and $h = 0.01$. We observe that the numerical solutions capture the profiles of the exact solutions quite well. Since we have not used any limiter, there are some localized oscillations near the singularities.

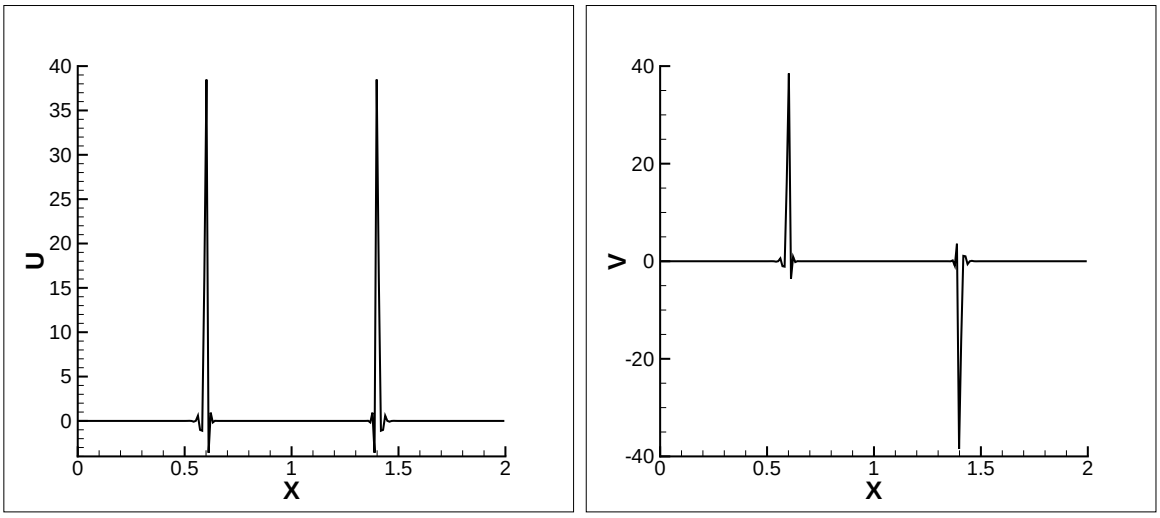

Figure 5.3: Solutions of u (left) and v (right) for (5.3) at $t = 0.4$.

5.2 Singular source term

Example 4. We solve the following problem

$$\begin{array}{ll} u_t + u_x = \delta(x-\pi), & (x,t) \in [0,2\pi] \times (0,1], \\ u(x,0) = \sin(x), & x \in [0,2\pi], \\ u(0,t) = 0, & t \in (0,1]. \end{array} \tag{5.4}$$

Clearly, the exact solution is

$$u(x,t) = \sin(x-t) + \chi_{[\pi,\pi+t]},$$

where $\chi_{[a,b]}$ denotes the indicator function of the interval $[a,b]$. We use the same time discretization as in the previous example, and use both $\mathcal{P}^1$ and $\mathcal{P}^2$ polynomials to approximate the exact solution on uniform meshes, then compute the L^2-norm of the error after post-precessing in the region away from the singularities at $t = 0.5$. In this example, we also take $d = 0.2$, and the region under consideration is $[0, \pi - 0.2] \cup [\pi + 0.2, \pi + 0.3] \cup [\pi + 0.7, 2\pi]$. In table 5.3, we can observe $(2k+1)$-th order convergence. The initial discretization is again obtained by taking the L^2 projection.

Moreover, figure 5.4 shows the numerical solutions with and without post-processing. We use $\mathcal{P}^2$ polynomials and take $h = 0.01$. From the figure we can observe the post-processor

Table 5.3: L^2-norm of the error between the numerical solution and the exact solution for equation (5.4) after post-processing in the region away from the singularity.

		$\mathcal{P}^1$ polynomial		$\mathcal{P}^2$ polynomial	
N	d	error	order	error	order
401	0.2	1.74E-06	-	4.29E-08	-
801	0.2	5.92E-09	8.22	6.80E-13	15.9
1601	0.2	7.36E-10	3.03	1.34E-17	12.3
3201	0.2	9.19E-11	3.01	3.86E-18	5.13
6401	0.2	1.15E-11	3.01	1.16E-19	5.07

does not smear the singularity too much and it can effectively damp out the the oscillations near the left singularity.

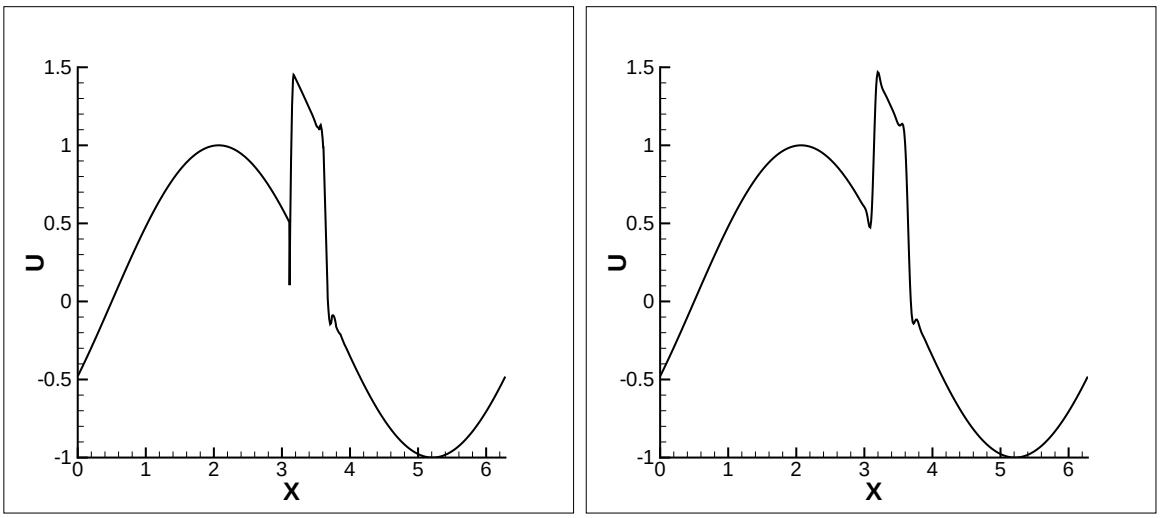

Figure 5.4: Numerical solutions for (5.4) at $t = 0.5$ with (right) and without (left) post-processing.

Example 5. We solve the following problem

$$\begin{aligned} &u_t + ((x+1)u)_x = \delta(x-c), && (x,t) \in [0, 1.5] \times (0, 1], \\ &u(x,0) = 0, && x \in [0, 1.5], \\ &u(0,t) = 0, && t \in (0, 1]. \end{aligned} \tag{5.5}$$

The exact solution is

$$u(x,t) = \frac{1}{1+x}[H(x-c) - H(x+1-(c+1)e^t)],$$

where $H(x)$ is the Heaviside function defined as

$$H(x) = \begin{cases} 0, & x < 0, \\ 1, & x \geq 0. \end{cases}$$

We take $c = \frac{\pi}{20}$ and compute the solution at $t = 0.5$ with $\mathcal{P}^1$ and $\mathcal{P}^2$ polynomials. Since $(x+1)$ is always positive, by using upwind fluxes, we always consider u_h^- to be the numerical flux at the cell interfaces. For time discretization, the classical fourth order Runge-Kutta method is used with $\Delta t = h^2$. In this example, we take $d = 0.1$, and the region under consideration is $[0, \frac{\pi}{20} - 0.1] \cup [\frac{\pi}{20} + 0.1, (\frac{\pi}{20} + 1)\sqrt{e} - 1.1] \cup [(\frac{\pi}{20} + 1)\sqrt{e} - 0.9, 1.5]$. In table 5.4, we can observe $(k+1)$-th and $(2k+1)$-th order convergence before and after post-processing respectively.

Table 5.4: L^2-norm of the error between the numerical solution with and the exact solution for equation (5.5) before and after post-processing in the region away from the singularity.

			$\mathcal{P}^1$ polynomial		$\mathcal{P}^2$ polynomial	
	N	d	error	order	error	order
before post-processing	400	0.1	7.08E-07	-	1.10E-08	-
	800	0.1	1.21E-07	2.56	4.37E-11	7.98
	1600	0.1	3.02E-08	2.00	5.46E-12	3.00
	3200	0.1	7.55E-09	2.00	6.83E-13	3.00
	6400	0.1	1.89E-09	2.00	8.53E-14	3.00
after post-processing	400	0.1	4.92E-07	-	8.65E-09	-
	800	0.1	7.49E-11	12.7	4.54E-14	17.5
	1600	0.1	7.43E-12	3.33	5.13E-19	16.4
	3200	0.1	9.31E-13	3.00	1.76E-20	4.86
	6400	0.1	1.16E-13	3.00	5.75E-22	4.94

Moreover, figure 5.5 shows the numerical solution with $\mathcal{P}^2$ polynomials and $h = 0.01$. We use the cell averages to plot the left panel of the figure. From the figure we can observe that the numerical solution agrees well with the exact solution away from the singularities. Since we have not used any limiter, there are some localized oscillations near the singularity on the right. It is interesting to observe that there are very few numerical oscillations near the left singularity. In the middle panel of figure 5.5, we use six Gaussian points to plot, and

the detailed zoom for the left singularity is given in the right panel. Clearly, the numerical solution only oscillates in the cell [0.15,0.16]. No oscillation is observed in the left figure for cell averages, and only one undershoot can be observed in the middle and right panels for which six Gaussian points are plotted. This can be explained by the size of the pollution region. In theorem 4.1, we have proved that, for such singularities, $\mathcal{R}_T$ contains only one cell. This implies that the numerical solution will oscillate within that cell, which clearly agrees with our observation.

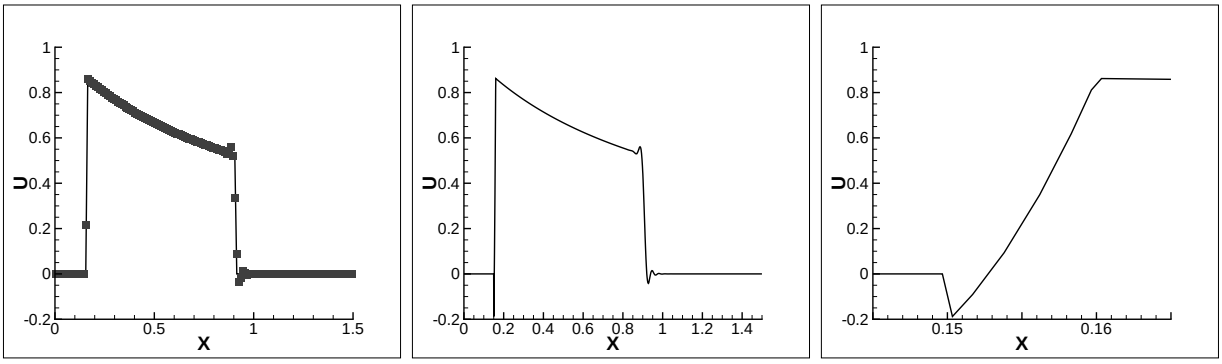

Figure 5.5: Numerical solutions for (5.5) at $t = 0.5$ plotted for the cell averages (left), six Gaussian points (middle) and the detailed zoom (right). In the left panel, the solid line is the exact solution and the symbols are the cell averages of the numerical solution.

5.3 Rendez-vous algorithm

Example 6. We solve the following problem

$$\begin{array}{ll} \rho_t + F_x = 0, & x \in [0,1], t > 0, \\ \rho(0,t) = u_0(x), & t > 0, \end{array} \tag{5.6}$$

where ρ is the density function, which is always positive. The flux F is given by

$$F(t,x) = v(t,x)\rho(t,x),$$

and the velocity v is defined by

$$v(t,x) = \int_{\mathbb{R}^n} (y-x)\xi(y-x)\rho(t,y)dy,$$

where $\xi(x)$ is a positive function and supported on a ball centered at zero with radius R. In [2] Canuto et al. investigated the discretized version of the PDE and proved that when t tends to infinity, the density function ρ will converge to some δ-singularities, and the distances between any of them cannot be less than R. Some computational results are shown in [2] based on a first order finite volume method. We consider $u_0(x) = 1$ and $\xi(x) = \chi_{[-R,R]}$ as an example. In figure 5.6, we apply the positivity-preserving limiter in [32] and use $\mathcal{P}^1$ polynomials, as well as the third order SSP Runge-Kutta discretization in time with $\Delta t = 0.1h$. In each time level, we first compute the value of v at the cell interfaces, then choose the numerical flux based on upwinding. Figure 5.6 shows the numerical approximation of $\rho(x)$ at $t = 1000$, with $h = 1/400$, $R = 0.02$ and zero boundary condition. We can observe 22 δ-singularities, agreeing with the numerical result in [2]. The algorithm is quite stable in this simulation. We observe that the $\mathcal{P}^1$ solution in the middle panel is more accurate than the $\mathcal{P}^0$ solution in the left panel, since the heights of the δ-singularities are almost doubled, which means less smearing of these singularities because the scheme is conservative. Moreover, we also plot in the right panel the detailed zoom of the middle one. We observe that there is no oscillation near the δ-singularities.

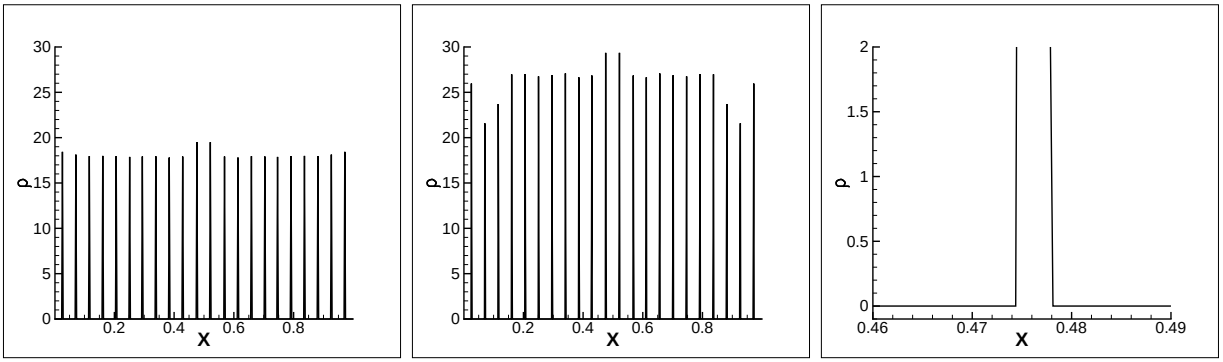

Figure 5.6: numerical density ρ for (5.6) at $t = 1000$ with $h = 1/400$ for example 4 when using $\mathcal{P}^0$ (left) and $\mathcal{P}^1$ (middle) polynomials. The right panel is the detailed zoom of the middle one.

6 Concluding remarks

In this paper, we use the discontinuous Galerkin (DG) method to solve hyperbolic conservation laws involving δ-singularities. We investigate the negative-order norm error estimates for the accuracy of the DG approximations to linear hyperbolic conservation laws with singular initial data or singular source terms. We also obtain error estimates in the L^2-norm after post-processing in one space dimension. Numerical experiments demonstrate that the rates of convergence we obtain are optimal. Numerical experiment with the nonlinear rendezvous problem illustrates the stability and good resolution of the DG method for nonlinear problems involving δ-singularities. The results in this paper give us evidence that the DG method is a good algorithm for problems involving δ-singularities in their solutions. In future work we will apply the DG method to more nonlinear hyperbolic equations involving δ-singularities.

References

[1] J.H. Bramble and A.H. Schatz, *High order local accuracy by averaging in the finite element method*, Mathematics of Computation, 31 (1977), 94-111.

[2] C. Canuto, F. Fagnani and P. Tilli, *An Eulerian approach to the analysis of Rendez-vous algorithms*, 17th IFAC World Congress 2008, M.J. Chung and P. Misra, editors, Volume 17, Part 1, Curran, Red Hook, New York, 2009.

[3] A. Chalaby, *On convergence of numerical schemes for hyperbolic conservation laws with stiff source terms*, Mathematics of Computation, 66 (1997), 527-545.

[4] P.G. Ciarlet, *Finite Element Method For Elliptic Problems*, North-Holland, Amsterdam, 1978.

[5] B. Cockburn, *A Introduction to the discontinuous Galerkin methods for convection dominated problems*, High-Order Method for Computational Physics (T. Barth and H. De-

conink, eds.), Lecture Notes in Computational Science and Engineering, vol. 9, Springer-Verlag Berlin Heidelberg, 1999, 69-224.

[6] B. Cockburn and J. Guzmán, *Error estimate for the Runge-Kutta discontinuous Galerkin method for the transport equation with discontinuous initial data*, SIAM Journal on Numerical Analysis, 46 (2008), 1364-1398.

[7] B. Cockburn, S. Hou and C.-W. Shu, *The Runge-Kutta local projection discontinuous Galerkin finite element method for conservation laws IV: the multidimensional case*, Mathematics of Computation, 54 (1990), 545-581.

[8] B. Cockburn, S.-Y. Lin and C.-W. Shu, *TVB Runge-Kutta local projection discontinuous Galerkin finite element method for conservation laws III: one-dimensional systems*, Journal of Computational Physics, 84 (1989), 90-113.

[9] B. Cockburn, M. Luskin, C.-W. Shu and E. Süli, *Enhanced accuracy by post-processing for finite element methods for hyperbolic equations*, Mathematics of Computation, 72 (2003), 577-606.

[10] B. Cockburn and C.-W. Shu, *TVB Runge-Kutta local projection discontinuous Galerkin finite element method for conservation laws II: general framework*, Mathematics of Computation, 52 (1989), 411-435.

[11] B. Cockburn and C.-W. Shu, *The Runge-Kutta discontinuous Galerkin method for conservation laws V: multidimensional systems*, Journal of Computational Physics, 141 (1998), 199-224.

[12] J.M. Greenberg, A.Y. Leroux, R. Baraille and A. Noussair, *Analysis and approximation of conservation laws with source terms*, SIAM Journal on Numerical Analysis, 34 (1997), 1980-2007.

[13] S. Gottlieb, C.-W. Shu and E. Tadmor, *Strong stability-preserving high-order time discretization methods*, SIAM Review, 43 (2001), 89-112.

[14] S. Hou and X.-D. Liu, *Solutions of multi-dimensional hyperbolic systems of conservation laws by square entropy condition satisfying discontinuous Galerkin method*, Journal of Scientific Computing, 31 (2007), 127-151.

[15] G.-S. Jiang and C.-W. Shu, *On a cell entropy inequality for discontinuous Galerkin methods*, Mathematics of Computation, 62 (1994), 531-538.

[16] F. John, *Partial different equations*, Springer-Verlag, New York, 1971

[17] C. Johnson, U. Nävert and J. Pitkäranta, *Finite element methods for linear hyperbolic problems*, Computer Methods in Applied Mechanics and Engineering, 45 (1984), 285-312.

[18] C. Johnson and J. Pitkäranta, *An analysis of the discontinuous Galerkin method for a scalar hyperbolic equation*, Mathematics of Computation, 46 (1986), 1-26.

[19] C. Johnson, A. Schatz and L. Walhbin, *Crosswind smear and pointwise errors in streamline diffusion finite element methods*, Mathematics of Computation, 49 (1987), 25-38.

[20] B. Koren, *A robust upwind discretization method for advection, diffusion and source terms*, Notes on Numerical Fluid Mechanics, 45, Vieweg, Braunschweig (1993), 117-138.

[21] R.J. LeVeque and H.C. Yee, *A study of numerical methods for hyperbolic conservation laws with stiff source terms*, Journal of Computational Physics, 86 (1990), 187-210.

[22] A. Noussair, *Analysis of nonlinear resonance in conservation laws with point sources and well-balanced scheme*, Studies in Applied Mathematics, 104 (2000), 313-352.

[23] P. de Oliveira and J. Santos, *On a class of high resolution methods for solving hyperbolic conservation laws with source terms*, Applied Nonlinear Analysis, 432-445, (Adélia

Sequeira, Hugo Beirão da Veiga, and Juha Hans Videman, eds.), Kluwer academic publishers, New York, Boston, Dordrecht, London, Moscow, 1999.

[24] W.H. Reed and T.R. Hill, *Triangular mesh methods for the Neutron transport equation*, Los Alamos Scientific Laboratory Report LA-UR-73-479, Los Alamos, NM, 1973.

[25] J.K. Ryan and B. Cockburn, *Local derivative post-processing for the discontinuous Galerkin method*, Journal of Computational Physics 228 (2009), 8642-8664.

[26] J.K. Ryan and C.-W. Shu, *On a one-sided post-processing technique for the discontinuous Galerkin methods*, Methods and Applications of Analysis, 10 (2003), 295-308.

[27] J. Santos and P. de Oliveira, *A converging finite volume scheme for hyperbolic conservation laws with source terms*, Journal of Computational and Applied Mathematics, 111 (1999), 239-251.

[28] H.J. Schroll and R. Winther, *Finite-difference Schemes for scalar conservation laws with source terms*, IMA Journal of Numerical Analysis, 16 (1996), 201-215.

[29] P.V. Slingerland and J.K. Ryan and C. Vuik *Position-dependent smooth-increasing accuracy-conserving (SIAC) filtering for improving discontinuous Galerkin solutions*, SIAM Journal on Scientific Computing, 33 (2011), 802-825.

[30] D. Walfisch, J.K. Ryan, R.M. Kirby and R. Haimes, *One-sided smoothness-increasing accuracy-conserving filtering for enhanced streamline integration through discontinuous fields*, Journal of Scientific Computing, 38 (2009), 164-184.

[31] Q. Zhang and C.-W. Shu, *Error estimates for the third order explicit Runge-Kutta discontinuous Galerkin method for linear hyperbolic equation in one-dimension with discontinuous initial data*, submitted to Numerische Mathematik.

[32] X. Zhang and C.-W. Shu, *On positivity preserving high order discontinuous Galerkin schemes for compressible Euler equations on rectangular meshes*, Journal of Computational Physics, 229 (2010), 8918-8934.

A Proof of lemma 3.1

In this appendix we prove lemma 3.1. The main line of proof is based on the idea in [6, 31]. For simplicity, we only consider δ-singularity in equation (1.2), hence $u_0(x) = \delta(x) + f(x)$, where $f(x)$ is sufficiently smooth and has a compact support on the computational domain Ω.

A.1 The weight function

Let $\varphi(x)$ be a positive bounded function, which can be taken as a weight function. For any function $q \in H_h^1$, we define the weighted L^2-norm as

$$\|q\|_{\varphi,D} = \left(\int_D q^2 \varphi dx \right)^{\frac{1}{2}}$$

in the domain D. If $\varphi = 1$ or $D = \Omega$, the corresponding subscript will be omitted.

In this paper, we will consider two weight functions $\varphi^1(x,t)$ and $\varphi^{-1}(x,t)$, respectively, in order to determine the left-hand and right-hand boundary of the region $\mathcal{R}_T$ such that, outside this region, we can resume the $(k+1)$-th order accuracy in the L^2-norm. Both weight functions are related to the cut-off of the exponent function $\phi(r) \in C^1 : \Omega \to \mathbb{R}$,

$$\phi(r) = \begin{cases} 2 - e^r, & r < 0, \\ e^{-r}, & r > 0, \end{cases}$$

and they are defined as the solutions of the linear hyperbolic problem,

$$\varphi_t^a + \varphi_x^a = 0, \tag{A.1}$$

$$\varphi^a(x,0) = \phi\left(\frac{a(x - x_c)}{\gamma h^\sigma} \right), \tag{A.2}$$

where $\gamma > 0$, $0 < \sigma < 1$ and x_c are three parameters which will be chosen later. We always assume $\gamma h^{\sigma-1} \geq 1$ in this section.

In [31], the authors have listed several properties about the two weight functions. Here, we state some of them that will be used.

Proposition A.1 *For each of the weight function $\varphi^a(x,t)$, the following properties hold*

$$1 \le \varphi^a(x,t) \le 2, \quad a(x - x_c - t) \le 0, \tag{A.3}$$

$$0 < \varphi^a(x,t) < h^s, \quad a(x - x_c - t) > s\ \log(1/h)\gamma h^\sigma. \tag{A.4}$$

Lemma A.1 *Let $\mathbb{V}$ be a Gauss-Radau projection, either $\mathbb{P}_-$ or $\mathbb{P}_+$. For any sufficiently smooth function $p(x)$, there exists a positive constant C independent of h and p, such that*

$$\|\mathbb{V}^\perp p\|_{\varphi,D} \le Ch^{k+1}\|\partial_x^{k+1} p\|_{\varphi,D}, \tag{A.5}$$

$$\|\mathbb{V}^\perp(\varphi v_h)\|_{\varphi^{-1},D} \le C\gamma^{-1}h^{1-\sigma}\|v_h\|_{\varphi,D}, \tag{A.6}$$

$$\|\mathbb{V}(\varphi v_h)\|_{\varphi^{-1},D} \le C\|v_h\|_{\varphi,D}. \tag{A.7}$$

where D is either the single cell I_j or the whole computational domain Ω.

Lemma A.2 *For any function $v \in V_h$ there holds the following identity*

$$\mathcal{H}(v,\varphi v) = -\frac{1}{2}\sum_j \varphi_{j+\frac{1}{2}}[v]^2_{j+\frac{1}{2}} + \frac{1}{2}(v,\varphi_x v). \tag{A.8}$$

A.2 The smooth solution

We consider the following problem

$$v_t + v_x = 0, \tag{A.9}$$

$$v(x,0) = v_0(x), \tag{A.10}$$

where the initial condition $v_0(x)$, is a sufficiently smooth function modified from the original initial condition $u_0(x) = \delta(x) + f(x)$ such that it agrees with $u_0(x)$ for all $x \in \Omega\backslash I_i$, and satisfies

$$|\partial_x^\alpha v_0(x)| \le Ch^{-\alpha-1}, \quad x \in I_i,$$

where I_i is the cell containing $x = 0$.

A.3 Error representation and error equations

Denote the error by $e = v - u_h$, where u_h approximates to equation (1.2) or equation(A.9). Clearly, e also satisfies the scheme (2.2) with $g(x,t) = 0$. We divide the error into the form $e = \eta - \xi$, where

$$\eta = v - \mathbb{P}_- v = \mathbb{P}_-^{\perp} v, \quad \text{and} \quad \xi = u_h - \mathbb{P}_- v.$$

Then following [31], we obtain

$$\begin{aligned}\frac{d\|\xi\|_\varphi^2}{dt} &= 2\left(\xi_t, \mathbb{P}_+^{\perp}(\varphi\xi)\right) + 2\left(\eta_t, \mathbb{P}_+(\varphi\xi)\right) + 2\mathcal{H}(\xi, \varphi\xi) - (\xi, \varphi_x\xi) \\ &= 2\Pi_1 + 2\Pi_2 - \Pi_3,\end{aligned}$$

where

$$\Pi_1 = \left(\xi_t, \mathbb{P}_+^{\perp}(\varphi\xi)\right), \quad \Pi_2 = \left(\eta_t, \mathbb{P}_+(\varphi\xi)\right), \quad \Pi_3 = \sum_j \varphi_{j+\frac{1}{2}} [\xi]_{j+\frac{1}{2}}^2.$$

First we estimate Π_1. Denote $w = \xi_t - \mathbb{P}_{k-1}\xi_t$. From the scheme (2.3), we have

$$(\xi_t, w)_j = (\eta_t, w)_j - (e_t, w)_j = (\eta_t, w)_j - [\xi]_{j-\frac{1}{2}} w_{j-\frac{1}{2}}^+.$$

Plugging the above into Π_1 and defining $\psi = \sqrt{\varphi}$, we obtain

$$\begin{aligned}(\xi_t, \mathbb{P}_+^{\perp}(\varphi\xi))_j &= \left(\frac{(\xi_t, w)_j}{\|w\|_{I_j}^2} w, \mathbb{P}_+^{\perp}(\varphi\xi)\right)_j \\ &= \left(\left((\eta_t, w)_j - [\xi]_{j-1/2} w_{j-\frac{1}{2}}^+\right) \frac{w}{\|w\|_{I_j}^2}, \mathbb{P}_+^{\perp}(\varphi\xi)\right)_j \\ &\le \frac{C}{\|w\|_{I_j}} \left(|(\psi\eta_t, w)_j| + \left|[\psi\xi]_{j-1/2} w_{j-\frac{1}{2}}^+\right|\right) \left\|\psi^{-1}\mathbb{P}_+^{\perp}(\varphi\xi)\right\|_{I_j} \\ &\le \frac{Ch^{1-\sigma}}{\gamma}\left(\|\eta_t\|_{\varphi,I_j}^2 + \|\xi\|_{\varphi,I_j}^2\right) + \frac{Ch^{1/2-\sigma}}{\gamma}\left(\varphi_{j-1/2}[\xi]_{j-1/2}^2 + \|\xi\|_{\varphi,I_j}^2\right).\end{aligned}$$

Summing up with respect to j, we obtain

$$(\xi_t, \mathbb{P}_+^{\perp}(\varphi\xi)) \le \frac{Ch^{1-\sigma}}{\gamma}\left(\|\eta_t\|_\varphi^2 + \|\xi\|_\varphi^2\right) + \frac{Ch^{1/2-\sigma}}{\gamma}\left(\sum_j \varphi_{j-1/2}[\xi]_{j-1/2}^2 + \|\xi\|_\varphi^2\right).$$

For Π_2, it is not difficult to find out that

$$\Pi_2 \le C\|\eta_t\|_\varphi \, \|\xi\|_\varphi \le C(\|\eta_t\|_\varphi^2 + \|\xi\|_\varphi^2).$$

Then if γ is large enough and $\sigma = \frac{1}{2}$, we have

$$2\Pi_1 + 2\Pi_2 - \Pi_3 \leq C\left(\|\eta_t\|_\varphi^2 + \|\xi\|_\varphi^2\right).$$

By Gronwall's inequality,

$$\|\xi(T)\|_\varphi^2 \leq C\int_0^T \|\eta_t\|_\varphi^2 dt + C\|\xi(0)\|_\varphi^2. \tag{A.11}$$

A.4 The final estimate

This part is almost the same as in [31]. We will only discuss the left-hand boundary of $\mathcal{R}_T$ since the discussion for the right one is similar. Denote $x_L(t) = t + x_c$ with

$$x_c = -2s\log(1/h)\gamma h^\sigma,$$

where s and γ are sufficiently large and $\sigma = 1/2$. As we have mentioned before, the δ-singularity in the initial datum is contained in the cell I_i. Then by proposition A.1, we obtain $0 < \phi(x) < h^s$ for any $x \in I_i$. We choose v_0 to satisfy $\mathbb{P}_k v_0 = \mathbb{P}_k u_0 = u_h(0)$, then

$$\|\xi(0)\|_\varphi \leq \|\xi(0)\|_{\varphi, L^2(\mathbb{R}\setminus I_i)} + \|\xi(0)\|_{\varphi, L^2(I_i)} \leq Ch^{k+1}\|f\|_{k+2} + Ch^{s-1/2}.$$

If s is large enough, then $\|\xi(0)\|_\varphi \leq Ch^{k+1}$.

Define the domain $\mathcal{R}_T^+ = (x_L(T), \infty)$, then

$$\|u_h - v\|_{\mathbb{R}\setminus\mathcal{R}_T^+} \leq \|u_h - v\|_{\varphi, \mathbb{R}\setminus\mathcal{R}_T^+} \leq \|\eta\|_{\varphi, \mathbb{R}\setminus\mathcal{R}_T^+} + \|\xi\|_\varphi \leq Ch^{k+1}\|f\|_{k+1} + \|\xi\|_\varphi.$$

To estimate the second term on the right hand side, we need to use (A.11). Denote

$$w(t) = \max\{x_{j+\frac{1}{2}} : x_{j-\frac{1}{2}} < t + \frac{1}{2}x_c, \forall j\},$$

and $\mathcal{R}_1(t) = (-\infty, w(t))$, $\mathcal{R}_2(t) = \mathbb{R}\setminus\mathcal{R}_1(t) = (w(t), \infty)$. If $\gamma h^{\sigma-1}$ is large enough, $\mathcal{R}_1(t)$ stays away from the bad interval $[t-h, t+h]$ where $v(x,t) \neq u(x,t)$, then we have

$$\|\eta_t\|_{\varphi, \mathcal{R}_1(t)} \leq Ch^{k+1}\|f\|_{k+2}.$$

Now we proceed to estimate $\|\eta_t\|_{\varphi,\mathcal{R}_2(t)}$. Since $\mathcal{R}_2$ contains the whole bad region, we will use the property of the weight function. By (A.4) we have $\varphi \leq h^s$ in this zone. Then we obtain

$$\|\eta_t\|_{\varphi,\mathcal{R}_2(t)} \leq Ch^{s/2}\|\eta_t\|_{\mathcal{R}_2(t)} \leq Ch^{s/2+k+1}\|\partial_x^{k+2}v\|_{\mathcal{R}_2(t)} \leq Ch^{(s-3)/2} + Ch^{s/2+k+1}\|f\|_{k+2,\mathcal{R}_2(t)}.$$

Similarly, we can estimate the right-hand side of the non-smooth region. If we take s large enough, we have

$$\|u_h - u(x,T)\|_{\mathbb{R}\setminus\mathcal{R}_T^+} = \|u_h - v(x,T)\|_{\mathbb{R}\setminus\mathcal{R}_T^+} \leq Ch^{k+1}\|f\|_{k+2} + Ch^{(s-3)/2} \leq Ch^{k+1}.$$